Research Article **Open Access**

Angela Handlovičová and Izabela Riečanová*

Numerical solution to the Complex 2D Helmholtz Equation based on Finite Volume Method with Impedance Boundary Conditions

DOI 10.1515/phys-2016-0044
Received Jun 08, 2016; accepted Oct 11, 2016

Abstract: In this paper, the numerical solution to the Helmholtz equation with impedance boundary condition, based on the Finite volume method, is discussed. We used the Robin boundary condition using exterior points. Properties of the weak solution to the Helmholtz equation and numerical solution are presented. Further the numerical experiments, comparing the numerical solution with the exact one, and the computation of the experimental order of convergence are presented.

Keywords: Helmholtz equation, Finite volume method, numerical solution, stability

PACS: 02.30.Jr, 47.11.Df

1 Introduction

Numerical methods in acoustics solve the wave equation

$$\frac{\partial^2 P}{\partial t^2} = c^2 \Delta P, \tag{1}$$

where P is the pressure and c is the speed of sound. This equation describes the behavior of sound, light, or water waves. In the case of time harmonic acoustic propagation and scattering [1], the pressure function is given by

$$P(x,t) = Re\left(A(x)e^{-i\omega t}\right). \tag{2}$$

Here $\omega = 2\pi f$ is the angular frequency measured in rad/s, f the frequency measured in Hz and Re denotes the real part. Function A is in general complex valued and is the complex acoustic pressure.

To solve (1), the method of separating the variables can be applied. Thus the time-independent form of the original equation is obtained, which is called the Helmholtz equation

$$\Delta A + k^2 A = 0. \tag{3}$$

Here $|A(x)|$ is the amplitude of the time harmonic pressure fluctuation at x and k is the acoustic wavenumber (number of radians per unit distance). Wavenumber is also given by the formula

$$k = \frac{\omega}{c}. \tag{4}$$

The Helmholtz equation is related to the problems of steady-state oscillations. The unknown function $A(x)$ is defined on a two or three dimensional domain D, where its boundary is denoted by ∂D. In our paper we focus on the most commonly relevant boundary condition [1], called impedance boundary condition of the type

$$\frac{\partial A}{\partial \mathbf{n}} + ik\beta A = g. \tag{5}$$

In this boundary condition $\mathbf{n}$ denotes the outward normal to the boundary ∂D, and $\frac{\partial}{\partial \mathbf{n}}$ denotes the normal derivative. The function g on the right side of the equation is identically zero in acoustic scattering problems [1], and is nonzero for the radiation problems. It is be generally considered as the sound source. β is the relative surface admittance. In general it is a function of position on the boundary and frequency. The simplest case is when the boundary is acoustically rigid or sound hard. In this case there is no flow across ∂D and $\beta = 0$, so we obtain Neumann boundary condition. If the value is set to $\beta = 1$, it means the boundary has maximum sound absorption, so the free space is considered. The results of simulations with changing values of β and g can be seen in [2].

Our main goal is to present a numerical scheme for solving the problem (3), (5) in 2D.

Angela Handlovičová: Department of Mathematics and Descriptive Geometry, Faculty of Civil Engineering, Slovak University of Technology in Bratislava, Bratislava, Slovakia; Email: handlovicova@math.sk
***Corresponding Author: Izabela Riečanová:** Department of Mathematics and Descriptive Geometry, Faculty of Civil Engineering, Slovak University of Technology in Bratislava, Bratislava, Slovakia; Email: riecanova@math.sk

2 Finite Volume Method

There are several numerical techniques for solving the Helmholtz equation. Among them we can mention the Finite element method e.g. in [3], or the Boundary element method e.g. in [4] and [5]. In this article we study numerical solution based on the Finite volume method which is an extension of the previous work [4].

We present the numerical scheme based on the Finite volume method [6]. The discretization of the domain D is the union of so called finite volumes (in 2D usually rectangles or triangles). This discretization is denoted as T_h, where the index h is connected with the size of finite volumes. In our case the domain will be a two dimensional rectangle and our finite volumes will be squares of size h. In each finite volume $p \in T_h$ we have a representative point X_p in which the approximated function can be evaluated. That is why our numerical solution is a piecewise constant function, which is constant on each finite volume, and is calculated at the representative point. This point is usually chosen in the barycentre of the finite volume. Moreover we denote by E the set of all edges of each finite volume $p \in T_h$. If we have our discretization as described above, our mesh fulfils an important property

$$X_p - X_q = d_{pq}\mathbf{n_{pq}} \tag{6}$$

for both neighbouring representative points X_p and X_q. Here $\mathbf{n_{pq}}$ is the outward normal of the finite volume p to the common side with finite volume q; this side is denoted by σ_{pq} and d_{pq} is the distance between representative points X_p and X_q. An important feature of the method is the local conservativity of numerical fluxes, which means that the flux is conserved from one discretization finite volume to its neighbour.

After the discretization of the domain we have n finite volumes along one side of the rectangle domain and m finite volumes along the other, a mesh of $m \times n$ finite volumes is obtained. The particular finite volume is labelled as p and its boundary as ∂p. In the finite volume we denote the constant value of the approximated solution as u_p, and the solution in the neighbouring volume as u_q. The size of the finite volume p is denoted by $m(p)$ and the edge σ_{pq} has the size denoted by $m(\sigma_{pq})$. We denote by $N(p)$ the set of all neighbours of the finite volume p, which means the finite volumes that have common side with volume p.

The finite volume numerical scheme can be obtained by integrating the differential equation (3) on each finite volume. Using Green's theorem we obtain

$$\int_p k^2 A dx + \int_{\partial p} \nabla A \cdot \mathbf{n} ds = 0. \tag{7}$$

We apply the approximation function as discussed above which can be denoted by

$$u_h(x) = u_p, \quad x \in p. \tag{8}$$

We use this property in (7) together with the approximation of the normal derivative by a standard finite difference. This way we obtain

$$k^2 u_p m(p) + \sum_{q \in N(p)} \frac{u_q - u_p}{d_{pq}} m(\sigma_{pq}) = 0. \tag{9}$$

The solution to the Helmholtz equation is based on complex values as

$$A = A^r + iA^i. \tag{10}$$

For the approximate solution it is the same

$$u_h = u_h^r + iu_h^i, \tag{11}$$

and analogously

$$u_p = u_p^r + iu_p^i, \tag{12}$$

where i is imaginary unit. Thus the proposed equation is valid for both real part and imaginary part. We will denote it in a similar way but with the upper indices "r" or "i". We have

$$\begin{aligned} k^2 u_p^r m(p) + \sum_{q \in N(p)} \frac{u_q^r - u_p^r}{d_{pq}} m(\sigma_{pq}) = 0, \\ k^2 u_p^i m(p) + \sum_{q \in N(p)} \frac{u_q^i - u_p^i}{d_{pq}} m(\sigma_{pq}) = 0. \end{aligned} \tag{13}$$

These equations are valid for the interior finite volumes.

We now denote by $E = E_{int} \cup E_{ext}$, where E_{int} is the set of all interior edges and E_{ext} is the set of all edges of all finite volumes that belong to ∂D. Further $T_h = T_{h,int} \cup T_{h,ext}$, where $T_{h,int}$ is the set of all finite volumes which have all edges in E_{int} and $T_{h,ext}$ is the set of all finite volumes that have at least one edge in E_{ext}. Finally by $N(p)_{int}$ we denote the set of those neighbours with common side $\sigma_{pq} \in E_{int}$, and $N(p)_{ext}$ is the set of neighbours with common side $\sigma_{pq} \in E_{ext}$.

From prescribed boundary condition (5), we obtained the conditions for the real and imaginary parts of the solution

$$\begin{aligned} \frac{\partial A^r}{\partial \mathbf{n}} - k\beta A^i = g^r, \\ \frac{\partial A^i}{\partial \mathbf{n}} + k\beta A^r = g^i \end{aligned} \tag{14}$$

For the finite volume $p \in T_{h,ext}$ we use the boundary conditions to approximate the numerical fluxes along the edges from $T_{h,ext}$. For this purpose we use exterior finite volumes

denoted by $qext$, and the value of the numerical solution at these finite volumes is denoted by u^r_{qext} and u^i_{qext}, respectively. Thus for $p \in T_{h,ext}$ we have

$$k^2 u^r_p m(p) + \sum_{q\in N(p)_{int}} \frac{u^r_q - u^r_p}{d_{pq}} m(\sigma_{pq}) + \sum_{qext\in N(p)_{ext}} \frac{u^r_{qext} - u^r_p}{d_{pqext}} m(\sigma_{pqext}) = 0,$$
$$k^2 u^i_p m(p) + \sum_{q\in N(p)_{int}} \frac{u^i_q - u^i_p}{d_{pq}} m(\sigma_{pq}) + \sum_{qext\in N(p)_{ext}} \frac{u^i_{qext} - u^i_p}{d_{pqext}} m(\sigma_{pqext}) = 0. \quad (15)$$

From (14) we obtain

$$\frac{u^r_{qext} - u^r_p}{d_{pqext}} - k\beta \frac{u^i_{qext} + u^i_p}{2} = g^r_{pq},$$
$$\frac{u^i_{qext} - u^i_p}{d_{pqext}} + k\beta \frac{u^r_{qext} + u^r_p}{2} = g^i_{pq}, \quad (16)$$

where g^r_{pq} and g^i_{pq} are values of real and imaginary part of prescribed boundary function g evaluated on the exterior edges belonging to $N(p)$ in the following way

$$g^r_{pq} = \frac{1}{m(\sigma_{pqext})} \int_{\sigma_{pqext}} g^r(s)ds,$$
$$g^i_{pq} = \frac{1}{m(\sigma_{pqext})} \int_{\sigma_{pqext}} g^i(s)ds. \quad (17)$$

Now, from equations (16), we eliminate the unknown values u^r_{eqxt} and u^i_{eqxt} that we substitute in the initial equations (15) in the numerical fluxes along the exterior edges. For more detailed description see section 4.

This way we create a system of linear algebraic equations, in which the matrix was of order $2nm$. After solving the system, both the real and imaginary part are obtained for each finite volume.

3 Properties of the Weak and Numerical Solution

Let the data in (5) fulfil the following assumptions

- $g = g^r + ig^i$ and $g^r \in L_2(\partial D)$, $g^i \in L_2(\partial D)$
- β is real number

Definition:

A complex valued function $A = A^r + iA^i$ is a **weak solution** of (3)-(5) if

- $A^r \in H^1(D))$ and $A^i \in H^1(D)$
- the following holds

$$\int_D \nabla A \nabla v dx = \int_{\partial D} (g + i\beta k A)\, v ds + k^2 \int_D A v dx \quad (18)$$
$$\forall v = v^r + iv^i,\ v^r \in H^1(D),\ v^i \in H^1(D)$$

If we now pose in (18) $v = \bar{A} = A^r - iA^i$, we immediately have

$$k^2 \left(||A^r||^2_{L_2(D)} + ||A^i||^2_{L_2(D)} \right) + \int_{\partial_D} \left(g_r A^r + g_i A^i \right) ds +$$
$$i \int_{\partial_D} \left(g^i A^r - g^r A^i \right) ds = ||\nabla A^r||^2_{L_2(D)} +$$
$$||\nabla A^i||^2_{L_2(D)} + i\beta k \int_{\partial_D} \left((A^r)^2 + (A^i)^2 \right) ds,$$

or

$$k^2 ||A||^2_{L_2(D)} + \int_{\partial_D} g\bar{A} ds = ||\nabla A||^2_{L_2(D)} + i\beta k ||A||^2_{L_2(\partial D)}. \quad (19)$$

We remind that the computational domain we assume in this section is rectangle, and our discretization mesh consists of squares with the edge of size h. We have m finite volumes along one direction of the domain D, and n along the another direction, so we have $n\times m$ finite volumes. Thus we have

$$m(p) = h^2,\ m(\sigma_{pq}) = h,\ d_{pq} = h.$$

We can express our numerical scheme in a similar way as it was done for the continuous equation. We obtain for $p \in T_{h,int}$

$$k^2 u_p h^2 + \sum_{q\in N(p)} (u_q - u_p) = 0, \quad (20)$$

and for $p \in T_{h,ext}$

$$k^2 u_p h^2 + \sum_{q\in N(p)_{int}} (u_q - u_p) + \sum_{qext\in N(p)_{ext}} (u_{qext} - u_p) = 0. \quad (21)$$

We can approximate the boundary condition by

$$\frac{u_{qext} - u_p}{h} + ik\beta u_{pq} = g_{pq}, \quad (22)$$

where

$$u_{pq} = \frac{u_{qext} + u_p}{2}.$$

Substituting $u_{qext} - u_p$ in (21) from (22) we have

$$k^2 u_p h^2 + \sum_{q\in N(p)_{int}} (u_q - u_p) + \quad (23)$$

$$\sum_{qext\in N(p)_{ext}} (g_{pq} - ik\beta u_{pq})\, h = 0.$$

Now we multiply each of the equation (20) and (21) by $\bar{u}_p = u_p^r - iu_p^i$, and add them together. Then for the second term using the usual finite volume property [6] we have

$$k^2 \sum_{p\in T_h} u_p^2 h^2 + \sum_{\sigma_{pq}\in E_{ext}} g_{pq}\bar{u}_p h = \sum_{\sigma_{pq}\in E_{int}} (u_q - u_p)^2 + ik\beta \sum_{\sigma_{pq}\in E_{ext}} u_{pq}\bar{u}_p h.$$

which can be rearranged in the form

$$k^2 \sum_{p\in T_h} u_p^2 h^2 + \sum_{\sigma_{pq}\in E_{ext}} g_{pq}\bar{u}_{pq} h = \sum_{\sigma_{pq}\in E_{int}} (u_q - u_p)^2 + ik\beta \sum_{\sigma_{pq}\in E_{ext}} u_{pq}^2 h + I,$$

where

$$I = \sum_{\sigma_{pq}\in E_{ext}} (g_{pq} - ik\beta u_{pq})\,(\bar{u}_{pq} - \bar{u}_p)h.$$

First we notice

$$(\bar{u}_{pq} - \bar{u}_p) = \frac{1}{2}(\bar{u}_{qext} - \bar{u}_p),$$

and using boundary approximation (22) for real and imaginary part we have

$$(\bar{u}_{pq} - \bar{u}_p) = \frac{1}{2}\bar{g}_{pq}h + ik\beta h\bar{u}_{pq}.$$

Thus for the term I we obtain

$$I = \frac{1}{2}h \sum_{\sigma_{pq}\in E_{ext}} (g_{pq} - ik\beta u_{pq})\,(\bar{g}_{pq}h + ik\beta h\bar{u}_{pq}) = \frac{1}{2}h \sum_{\sigma_{pq}\in E_{ext}} \left(g_{pq}^2 + k^2\beta^2 u_{pq}^2 + 2k\beta\left(g_{pq}^r u_{pq}^r - g_{pq}^i u_{pq}^i\right)h\right).$$

Now we use the discrete H^1 seminorm defined in [6]

$$||u||_{1T_h} = \left(\sum_{\sigma\in E_{int}} \frac{m(\sigma)}{d_\sigma}(D_\sigma u)^2\right)^{\frac{1}{2}}, \tag{24}$$

where $D_\sigma u = |u_p - u_q|$, $\sigma = \sigma_{pq}$. If we now use the definition of a constant numerical solution (8), we can write

$$k^2||u_h||^2_{L_2(D)} + \sum_{\sigma_{pq}\in E_{ext}} g_{pq}\bar{u}_{pq}h = ||u_h^r||^2_{1T_h} + ||u_h^i||^2_{1T_h} + ik\beta \sum_{\sigma_{pq}\in E_{ext}} u_{pq}^2 h + \frac{h}{2}\sum_{\sigma_{pq}\in E_{ext}} \left(g_{pq}^2 + k^2\beta^2 u_{pq}^2 + 2k\beta\left(g_{pq}^r u_{pq}^r - g_{pq}^i u_{pq}^i\right)\right)h. \tag{25}$$

4 Numerical Scheme for Regular Mesh

We use the same computational domain as in the previous section. Now we derive numerical schemes for the real and imaginary part of the complex valued approximation function.

We have two types of the linear algebraic equations. The first belongs to the finite volumes from the set $T_{h,int}$, and second for the finite volumes from the set $T_{h,ext}$. In the first case we have for both, real and imaginary part of the numerical solution, the following equations

$$\begin{aligned} k^2 u_p^r h^2 + \sum_{q\in N(p)} (u_q^r - u_p^r) &= 0, \\ k^2 u_p^i h^2 + \sum_{q\in N(p)} (u_q^i - u_p^i) &= 0. \end{aligned} \tag{26}$$

For the second case we have some sides (one or two) of the finite volume that belongs to the boundary of the domain D. Here we use the boundary condition and the approximation described above

$$\begin{aligned} \frac{u_{qext}^r - u_p^r}{h} - k\beta\frac{u_{qext}^i + u_p^i}{2} &= g_{pq}^r, \\ \frac{u_{qext}^i - u_p^i}{h} + k\beta\frac{u_{qext}^r + u_p^r}{2} &= g_{pq}^i. \end{aligned} \tag{27}$$

From these equations we can easily eliminate the unknown values u_{qext}^r, u_{qext}^i:

$$u_{qext}^r = \frac{4hg_{pq}^r + 2h^2k\beta g_{pq}^i + 4hk\beta u_p^i + (4 - h^2k^2\beta^2)u_p^r}{4 + h^2k^2\beta^2},$$

$$u_{qext}^i = \frac{4hg_{pq}^i - 2h^2k\beta g_{pq}^r + (4 - h^2k^2\beta^2)u_p^i - 4h\beta k u_p^r}{4 + h^2k^2}.$$

Substituting these values into (15) for $p \in T_{h,ext}$ we have

$$\begin{aligned} k^2 u_p^r h^2 + \sum_{q\in N(p)_{int}} (u_q^r - u_p^r) + \\ \sum_{qext\in N(p)_{ext}} \left(Au_p^r - Bu_p^i + Cg_{pq}^r + Dg_{pq}^i\right) = 0, \\ k^2 u_p^i h^2 + \sum_{q\in N(p)_{int}} (u_q^i - u_p^i) + \\ \sum_{qext\in N(p)_{ext}} \left(Au_p^i + Bu_p^r + Cg_{pq}^i - Dg_{pq}^r\right) = 0, \end{aligned} \tag{28}$$

where

$$A = \frac{-4 + k^2h^2\beta^2}{4 + k^2\beta^2h^2}, \quad B = \frac{4k\beta^2 h}{4 + k^2\beta^2h^2}, \quad C = \frac{4h}{4 + k^2\beta^2h^2}, \quad D = \frac{2k\beta^2h^2}{4 + k^2\beta^2h^2}. \tag{29}$$

In this way we obtain linear system of algebraic equation with unknowns u_p^r, u_p^i, $p \in T_h$.

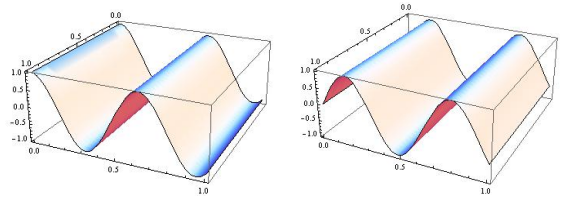

Figure 1: Exact solution (left real part, right imaginary part) for the wavenumber $10rad/m$

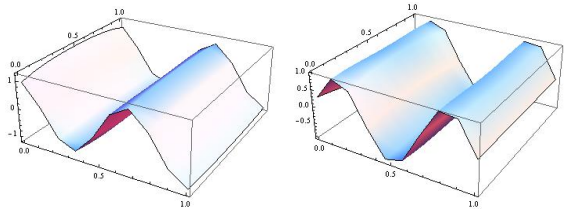

Figure 2: Numerical solution (left real part, right imaginary part) for the wavenumber $10rad/m$, $n = 10$

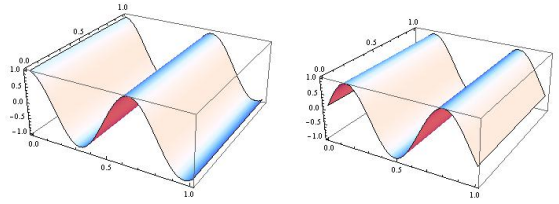

Figure 3: Numerical solution (left real part, right imaginary part) for the wavenumber $10rad/m$, $n = 40$

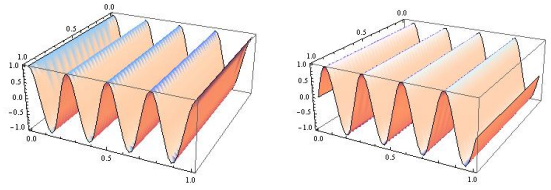

Figure 4: Exact solution (left real part, right imaginary part) for the wavenumber $25rad/m$

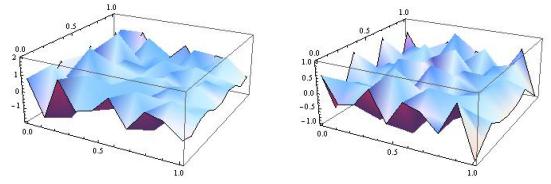

Figure 5: Numerical solution (left real part, right imaginary part) for the wavenumber $25rad/m$, $n = 10$

5 Numerical experiments

This section describes the results of the code, which solves the Helmholtz equation by the Finite volume method on the square domain of size 1 metre.

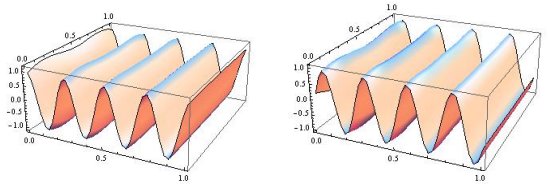

Figure 6: Numerical solution (left real part, right imaginary part) for the wavenumber $25rad/m$, $n = 40$

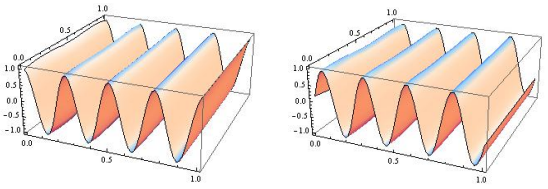

Figure 7: Numerical solution (left real part, right imaginary part) for the wavenumber $25rad/m$, $n = 60$

5.1 Experiment 1 - boundary conditions with $\beta = 1$

First to be presented is the solution of (3)-(5) with $\beta = 1$ in (5), so Robin boundary conditions are prescribed for all sides of domain. For the beginning we must use the exact solution used in [3]

$$u(x, y) = e^{i(k_1 x + k_2 y)} = \cos(k_1 x + k_2 y) + i \sin(k_1 x + k_2 y), \tag{30}$$

where the values k_1, k_2 are given by

$$k_1 = k \cos\theta, \quad k_2 = k \sin\theta. \tag{31}$$

The source function g was set so as to comply with the exact solution (30). Firstly we present results for $\theta = \frac{\pi}{2}$, for two different wavenumbers. Figure 1 shows the exact solution for $k = 10rad/m$, extra for real and imaginary part.
Figure 2 depicts the numerical solution to the Helmholtz equation for the number of discretizing points $n = 10$ (i.e. 100 finite volumes), and the Figure 3 for $n = 40$. It is clear that with the finer discretization the results are more accurate.

Next figures are dedicated to the bigger wavenumber. It is known that higher frequencies (i.e. bigger wavenumbers) require finer discretization, if we want to get results close to the exact solution [7]. Figure 4 shows the exact solution for the wavenumber $25rad/m$.
Figures 5 and 6 depict the numerical solution for 10 and 40 discretizing points.
It is clear that it is more difficult to approximate this function. Figure 7 shows plots for $n = 60$, where the results get very close to the exact solution.

Table 1: Values of the L2 error, $\theta = \frac{\pi}{2}$

	$k = 10rad/m$			$k = 25rad/m$		
n	10	40	60	10	40	60
L2 error	0.2653	0.0143	0.0063	1.3518	0.2324	0.1000

Table 2: Values of EOC for the wavenumber $10rad/m$, $\theta = \frac{\pi}{2}$

n	L2 error	α
10	0.265255	2.17192
20	0.058864	2.03935
40	0.014320	2.01011
80	0.003555	

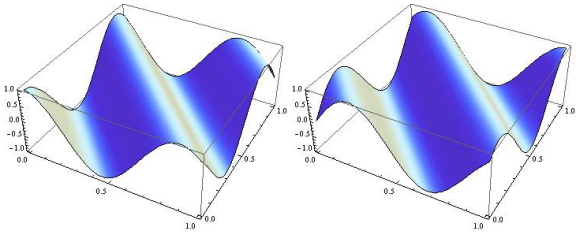

Figure 8: Exact solution (left real part, right imaginary part) for the wavenumber $10rad/m$

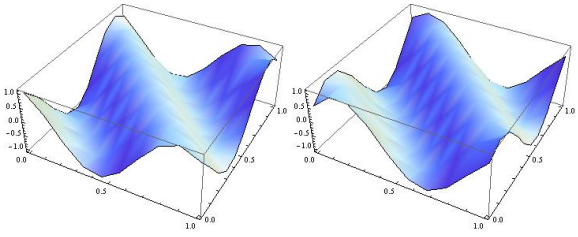

Figure 9: Numerical solution (left real part, right imaginary part) for the wavenumber $10rad/m$, $n = 10$

The L2 error was calculated by the formula

$$\sqrt{\sum((u_p^r - u_{exact}^r)^2 m(p)^2 + (u_p^i - u_{exact}^i)^2 m(p)^2)}. \quad (32)$$

Here u_p^r and u_p^i are the numerically calculated values. u_{exact}^r and u_{exact}^i are the precise values calculated from the exact solution. Table 1 shows the values.

The experimental order of convergence was calculated using the formula

$$L2\ error_h < Ch^\alpha, \quad (33)$$

where h is the length of the finite volume. α will be then calculated by

$$\alpha = \log_2 \frac{L2\ error_h}{L2\ error_{2h}} \quad (34)$$

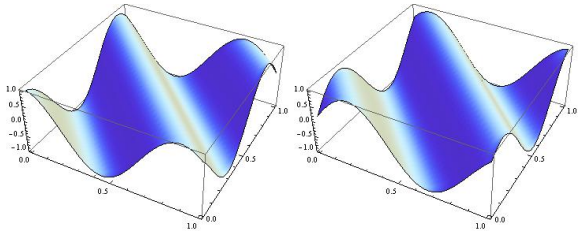

Figure 10: Numerical solution (left real part, right imaginary part) for the wavenumber $10rad/m$, $n = 40$

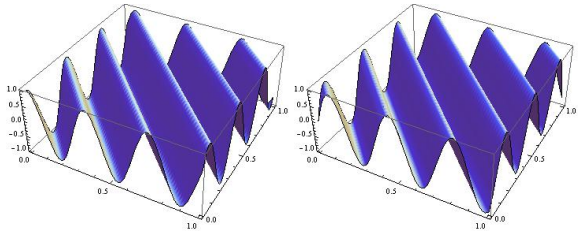

Figure 11: Exact solution (left real part, right imaginary part) for the wavenumber $25rad/m$

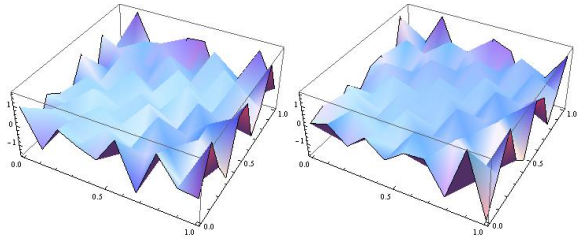

Figure 12: Numerical solution (left real part, right imaginary part) for the wavenumber $25rad/m$, $n = 10$

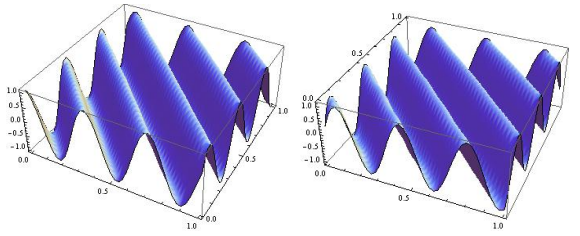

Figure 13: Numerical solution (left real part, right imaginary part) for the wavenumber $25rad/m$, $n = 40$

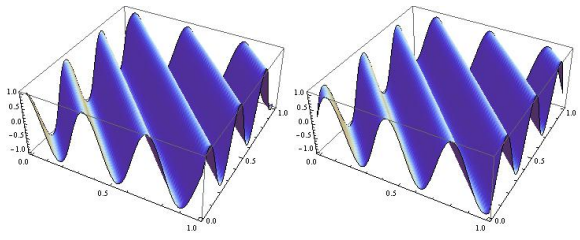

Figure 14: Numerical solution (left real part, right imaginary part) for the wavenumber $25rad/m$, $n = 60$

Table 3: Values of the L2 error, $\theta = \frac{\pi}{4}$

	$k = 10rad/m$			$k = 25rad/m$		
n	10	40	60	10	40	60
L2 error	0.1425	0.0082	0.0036	1.5407	0.1238	0.0541

Table 4: Values of EOC for the wavenumber $10rad/m$, $\theta = \frac{\pi}{4}$

n	L2 error	α
10	0.142520	
		2.09584
20	0.033340	
		2.02356
40	0.008200	
		2.00635
80	0.002041	

and from the theory it is known that its value is expected to be converging to 2. Table 2 shows the results for the wavenumber $10rad/m$.

Next figures 8 - 14 are for the value of $\theta = \frac{\pi}{4}$. First we show the exact solution and the results of the numerical experiments for the wavenumber $10rad/m$ (Figure 8 - 10). Lastly, figures 11 - 14 depict the solutions for the wavenumber $25rad/m$.
Presented figures and tables (3 and 4) show, that the behaviour is very similar to the previous value of θ.

5.2 Experiment 2 - mixed boundary conditions

The final part of the paper shows the results of program with changed boundary conditions. The domain is divided in two parts

$$\partial D = \partial D_{Robin} \cup \partial D_{Neumann}. \tag{35}$$

The boundary conditions on three sides of the boundary ∂D_{Robin} are prescribed as in the previous case, where $\beta = 1$ in (5). For part of the right side of the domain

$$\partial D_{Neumann} = \partial D \setminus \partial D_{Robin}, \tag{36}$$

$$\partial D_{Neumann} = \{[x, y] \in \partial\Omega; x = 1; 0.25 < y, 0.75\}, \tag{37}$$

the value of $\beta = 0$ in (5), so zero Neumann boundary conditions were obtained

$$\frac{\partial A}{\partial \mathbf{n}} = 0. \tag{38}$$

This combination of Robin and Neumann boundary conditions can represent for example a column (i.e. a hard wall barrier) standing in the free space. Exact solution is the same as in the previous case (30). The following tables 5 and 6 show the values of L2 error and EOC.

Table 5: Values of the L2 error for case with changed boundary conditions, $\theta = \frac{\pi}{2}$

	$k = 10rad/m$			$k = 25rad/m$		
n	10	40	60	10	40	60
L2 error	0.2757	0.0150	0.0066	1.2876	0.2376	0.1024

Table 6: Values of EOC for the wavenumber $10rad/m$ for the case with changed boundary conditions, $\theta = \frac{\pi}{2}$

n	L2 error	α
10	0.275654	
		2.15734
20	0.061793	
		2.04152
40	0.015010	
		2.01061
80	0.003725	

6 Conclusion

We have studied the numerical solution to the Helmholtz complex-valued equation. Our numerical solution is obtained using classical Finite volme method. For discretization of the boundary condition, which is of Robin type, we have used aditional exterior finite volumes by eliminating values on them. Properties of the weak solution and numerical solution are derived. Numerical experiments of various cases with changing boundary conditions show experimental order of convergence for the numerical solution to the exact one.

Acknowledgement: This work was supported by VEGA 1/0728/15.

References

[1] Chandler-Wild S., Langdon S., Boundary element methods for acoustics, Lecture notes, University of Reading, Department of Mathematics, 2007

[2] Handlovičová A., Riečanová I., Roozen N. B., Rigid piston simulations of acoustic space based on Finite volume method, Proceedings of Aplimat, 15-th Conference on Applied Mathematics, Institute of Mathematics and Physics, Faculty of Mechanical Engineering STU in Bratislava, 2016, ISBN 978-80-227-4531-4

[3] Babuška I. M., Ihlenburg F., Paik E. T., Sauter S. A., A Generalized Finite Element Method for Solving the Helmholtz Equation in

two Dimensions with Minimal Pollution, Comput. Methods Appl. Mech. Engrg. 128, 1995, 325-359

[4] Riečanová I., Finite volume method scheme for the solution of Helmholtz equation, Proceedings of Aplimat, 14-th Conference on Applied Mathematics, Institute of Mathematics and Physics, Faculty of Mechanical Engineering STU in Bratislava, 2015, ISBN 978-80-227-4314-3

[5] Sauter S. A., Schwab C., Boundary Element Methods, Springer-Verlag, Berlin, 2011, 561

[6] Eymard R., Gallouet T., Herbin R., Finite Volume Methods, Handbook of Numerical Analysis, Elsevier, 2007

[7] Riečanová I., Solution of the Helmholtz equation by the Boundary element method and the Finite volume method, Proceedings of Advances in Architectural, Civil and Environmental Engineering, faculty of civil Engineering, Slovak University of Technology in Bratislava, 2014, 29-36, ISBN 978-80-227-4301-3